Sensors and Actuators B 203 (2014) 54–62

Contents lists available at ScienceDirect

Sensors and Actuators B: Chemical

journal homepage: www.elsevier.com/locate/snb

Multi-fluorescent micro-sensor for accurate measurement of pH and temperature variations in micro-environments

Hengjun Liu [a,*], Hisataka Maruyama [a], Taisuke Masuda [a], Ayae Honda [b], Fumihito Arai [a]

[a] Department of Micro-Nano Systems Engineering, Nagoya University, Nagoya 464-8603, Japan
[b] Department of Frontier Bioscience, Hosei University, Tokyo 192-0982, Japan

ARTICLE INFO

Article history:
Received 16 January 2014
Received in revised form 18 June 2014
Accepted 23 June 2014
Available online 28 June 2014

Keywords:
Fluorescein isothiocyanate (FITC)
Rhodamine B
Amino-polystyrene microbeads (Ps)
pH sensitivity
Temperature compensation

ABSTRACT

In this study, a novel multi-fluorescent micro-sensor that can respond to both pH and temperature was designed and synthesized. It is based on amino-polystyrene microbeads, and two different fluorescent indicators (Rhodamine B and Fluorescein isothiocyanate) were used simultaneously to synthesize the fluorescent micro-sensor. Rhodamine B was embedded inside the amino-polystyrene microbeads, whereas Fluorescein isothiocyanate (FITC) was used to modify the surface of the beads. Because of the different fluorescence wavelengths and measurement positions of FITC and Rhodamine B, interference from each fluorescent indicator should be avoided. The fluorescence responses of FITC and Rhodamine B to pH and temperature, respectively, were detected. Rhodamine B demonstrates an excellent linear relationship between relative fluorescence intensity and temperature, while the relative fluorescence intensity was found to be independent of the pH. The calibrated sensitivity of Rhodamine B is −3.4%/°C, with a temperature accuracy of 0.1 °C. Therefore, changes in the temperature information can be calibrated based on the relative fluorescence intensity changes in Rhodamine B. On the other hand, FITC is sensitive to both pH and temperature. We propose a temperature compensation method for pH calibration. After temperature compensation, the pH accuracy calibrated based on the pH sensitivity of FITC improves from 1.5 to 0.2.

1. Introduction

Research has proven that temperature plays an important role in many cellular events, and has close relationships with cell state and cellular functions [1]. The intracellular pH modulates the function of many organelles and plays a pivotal role in many physiological and pathological processes [2,3]. Therefore, measurements of temperature and intracellular and extracellular pH can provide critical information on cell activities. For instance, in the case of cancer cells and several other physiological events, the rate of heat production rises [4] and the cellular pH is known to become lower [5,6] than that of normal cells. Therefore, the development of micro- and biocompatible sensors that can reveal temperature and pH changes in cells has become an urgent demand.

Many types of micro-sensors for physiological cell conditions have been developed and include electrical, chemical, and fluorescent sensors. Small molecular fluorescent probes have been widely used for cell detection, and fluorescence measurements such as fluorescence intensity and lifetimes are two of the most promising methods for on-chip cell analysis [7–10]. However, the widely used small-molecule indicators typically possess problems such as fast leakage, lack of membrane permeability, poor photostability, or sensitivity to ionic strength [11], and these problems have limited their practical applications. To overcome this, fluorescence-based microbeads have potential as sensors in medicine and biotechnology, especially since multiple indicators can be attached to a single particle. However, the effect of other conditions on sensitivity to the target condition has not been sufficiently considered [12]. For example, many pH chemical sensors were investigated based on the fluorescence property of fluorescein isothiocyanate (FITC) [13,14], but the sensitivity of FITC to temperature was not adequately considered. Additionally, no fluorescent micro-sensors that can simultaneously detect pH and temperature changes in their surroundings have been reported.

In this paper, we have synthesized a novel multi-fluorescent micro-sensor based on polymeric microbeads which can respond to

* Corresponding author at: Nagoya University, Furo-cho, Chikusa-ku, Nagoya 464-8603, Japan. Tel.: +81 52 789 5026; fax: +81 52 789 5027.
E-mail addresses: dengxr_1@hotmail.com (H. Liu), hisataka@mech.nagoya-u.ac.jp (H. Maruyama), masuda@mech.nagoya-u.ac.jp (T. Masuda), ayhonda@hosei.ac.jp (A. Honda), arai@mech.nagoya-u.ac.jp (F. Arai).

http://dx.doi.org/10.1016/j.snb.2014.06.079
0925-4005/

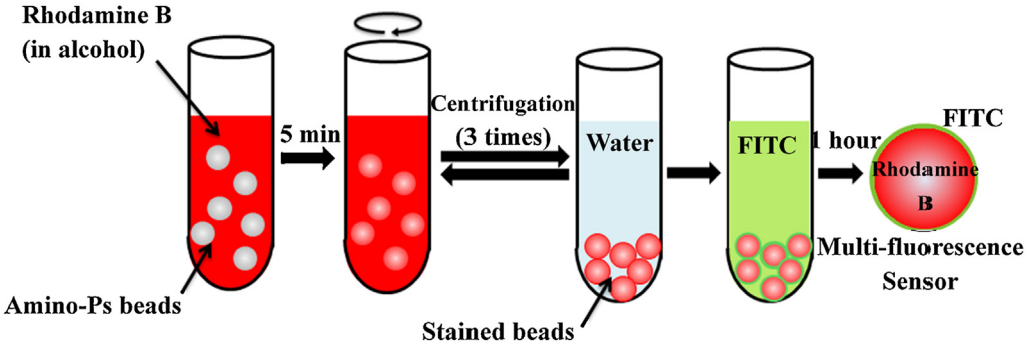

Fig. 1. Schematic illustration of the synthetic process for the multi-fluorescent sensor.

both pH and temperature change of the surroundings. Two different kinds of fluorescent dyes (Rhodamine B and FITC) are introduced to a single microbead simultaneously, but the positions of FITC and Rhodamine B are different. So any interference from each fluorescent dye is expected to be negligible by this method. Fluorescence microscopy is used to monitor fluorescent probes which can provide a high signal to noise ratio and a good spatial and temporal resolution. Fluorescence responses of Rhodamine B and FITC to both pH and temperature are studied and the temperature sensitivity and pH sensitivity of the micro-sensor are calibrated. And then based on the sensitivities of the micro-sensor, temperature change and pH change of surroundings have been calibrated. Moreover, a method of temperature compensation for pH calibration is proposed and the accuracy of the micro-sensor for pH and temperature calibrations is also discussed.

2. Materials and methods

2.1. Synthesis of the multi-fluorescent micro-sensor

Polystyrene (Ps) microbeads (1 μm in diameter) with amino group modified surfaces were used as the sensor carriers. Rhodamine B was embedded inside the amino-polystyrene beads, and FITC was modified on the surface of the beads as shown in Fig. 1. First, a solution of amino-polystyrene beads and 1 g/L Rhodamine B (in alcohol) (1:1 v/v) was stirred for 5 min and then washed with deionized (DI) water. The Ps beads swell in the presence of alcohol allowing Rhodamine B to get into and stain the beads inside. The expanded Ps beads shrink after washing with DI water. Then, the beads were added to a FITC saturated aqueous solution for 1 h and followed by three washes with DI water. FITC was immobilized on the surface of the amino-polystyrene beads through the chemical reaction shown in Fig. 2. The positions of FITC and Rhodamine B are different so any interference from each fluorescent dye is expected to be negligible.

2.2. Experimental systems

The fluorescent image of the target is obtained from an inverted confocal microscope (Ti-E Nikon) equipped with a high magnification lens (Plan Fluor 100×, Nikon) and CCD camera (iXon ultra, Andoe). The experimental system for fluorescence measurement is shown in Fig. 3. The excitation wavelengths of FITC are in the range of 405–525 nm, and it always has a strong absorbance at 488 nm. The excitation wavelengths of Rhodamine B are in the range of 500–590 nm, and it always has a strong absorbance at 561 nm. Therefore, wavelengths of 488 and 561 nm were selected as the excitation wavelengths for FITC and Rhodamine B, respectively.

Intensity based fluorescence measurements depend on many parameters, and the fluorescence intensity is represented in Eq. (1) [15].

$$I(t) = I_0{}'C\Phi\varepsilon \exp(-\varepsilon x C) \times \exp\left(\frac{-t}{\tau}\right) \quad (1)$$

where I (W/m^3) is the optical energy emitted from the fluorescent material per unit time, $I_0{}'$ (W/m^3) the excitation light flux on the fluorescent material, C (g/m^3) is the concentration of the fluorescent material, Φ the fluorescence quantum yield, and ε is the absorbance index. Φ decreases with environmental variation, whereas ε has low environmental dependence. x (m) is the propagation distance in the material. τ (s) is fluorescence lifetime. t (s) is the excitation time.Φ is variable depending on environmental conditions such as temperature, pH, and ions.

The laser source is class 3B laser with a laser power of 50 mW and a high stability of ±0.5% h^{-1}. The variation of dye amount from bead to bead is within 5%. Electron-multiplying gain is set to 200×, and the exposure time for one fluorescent image is 200 ms. So the fluorescence intensity measurement is mainly dependent on Φ. The lasers are controlled using a laser confocal scanning unit (CSU-X1, Yokogawa). The motorized filter changer model is available which make it easy to change the laser channel between 488 and 561 nm. The X–Y stage (BIOS-105 T, Sigma Koki) of the microscope was controlled by the stepping motors, and the Z axis was controlled by the stepping motor.

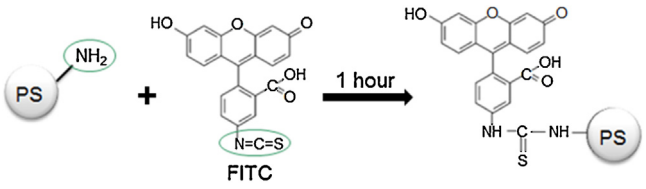

Fig. 2. Process for FITC assembly on the amino-polystyrene beads.

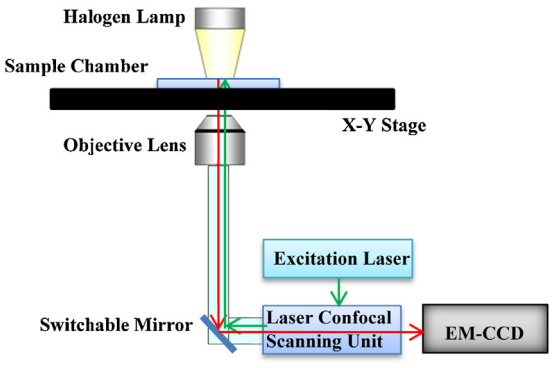

Fig. 3. Schematic of the inverted confocal microscopy system.

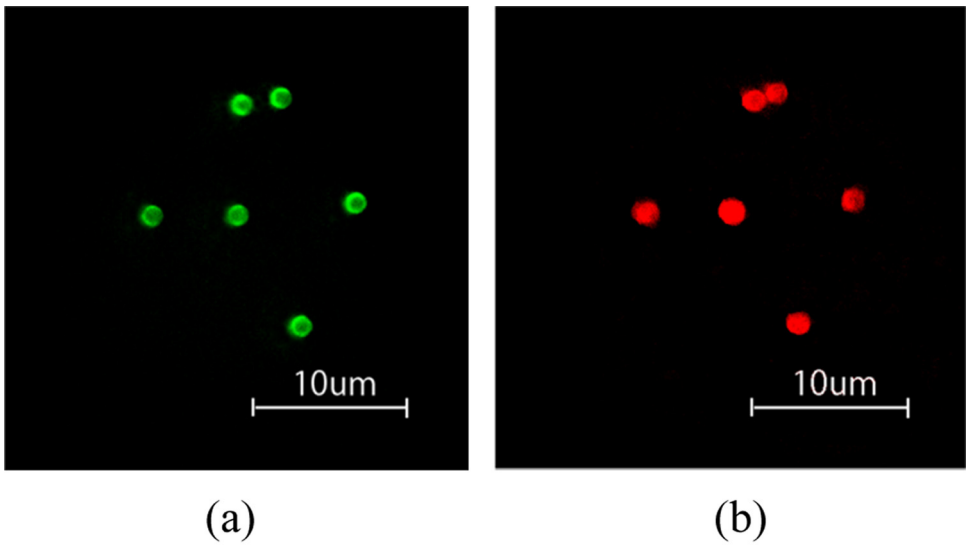

Fig. 4. Fluorescent images for indicators (a) FITC (excited at 488 nm) and (b) Rhodamine B (excited at 561 nm).

2.3. Measurement methods of the micro-sensor

We studied the fluorescence responses of the micro-sensor to different pH values and temperatures. Buffer solutions with different pH values (pH 5–8) were prepared. An incubation chamber was used to maintain the sample temperature, and the incubator chamber had four heaters (top heater, bath heater, stage heater, and lens heater). The temperature was controlled in the range of 32–38 °C.

After the microbeads were stained with Rhodamine B and FITC, 3 mL of the bead solution was added to a glass dish and kept in the dark until the beads adhered to the bottom of the dish (almost 10 h). Then the dish was placed in the incubation chamber, and the top of incubation chamber was covered to avoid any interference from the lights. The fluorescence intensity of the beads was measured using a fluorescence microscope. The stability and fluorescence responses of the micro-sensor to pH and temperature, its fluorescence reversibility, and its endurance in the surrounding ionic strength were all detected. For the fluorescence measurements of the micro-sensor response to pH and temperature, the sample temperature was increased from 32 to 38 °C in a pH 5 solution. Then the pH was changed to 6, 7, 8, and the fluorescence responses to temperature (32–38 °C) were repeatedly measured. We kept detecting the same beads during the experiments.

3. Results and discussion

3.1. Stability of the multi-fluorescent micro-sensor

Fig. 4 shows the fluorescent images of the micro-sensor. Green fluorescence detected at ex. 488 nm from FITC and red fluorescence detected at ex. 561 nm from Rhodamine B was observed. Before measuring the fluorescence responses of the micro-sensor to pH and temperature, the stability of the sensor was detected for 5 days. The pH value of the bead solution was 7.4 and the chamber temperature was set to 34 °C. After the beads adhered to the bottom of the dish, the fluorescence intensity was detected every 24 h for 5 days. We detected the same ten beads during the experiment and the fluorescence intensity results shown in Fig. 5 are the average values of the ten beads. There is almost no change in the fluorescence intensity for both Rhodamine B and FITC, suggesting the bead possesses a high stability without Rhodamine B diffusion in at least 5 days. Actually, we preserved the redundant sensor for more than 2 weeks and the fluorescence intensity of Rhodamine B was almost same as its initial value. The variation of intensity over different beads is within 5%.

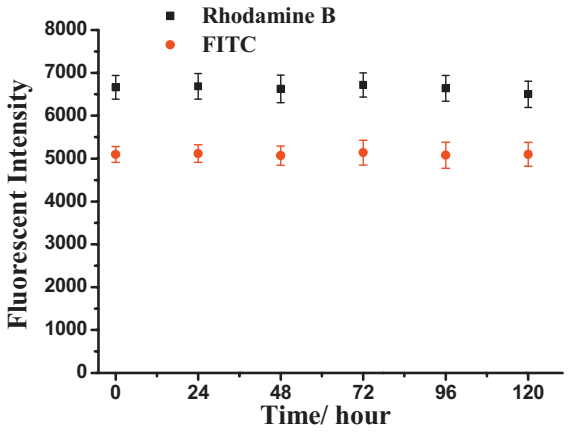

Fig. 5. Fluorescence stability of the sensors over 5 days. (pH 7.4, 34 °C).

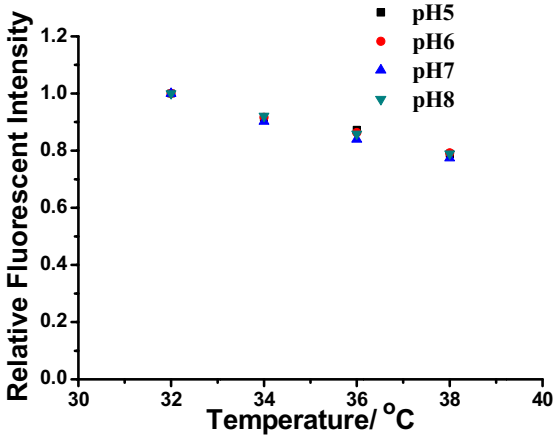

Fig. 6. The response of Rhodamine B to temperature at different pH (5–8).

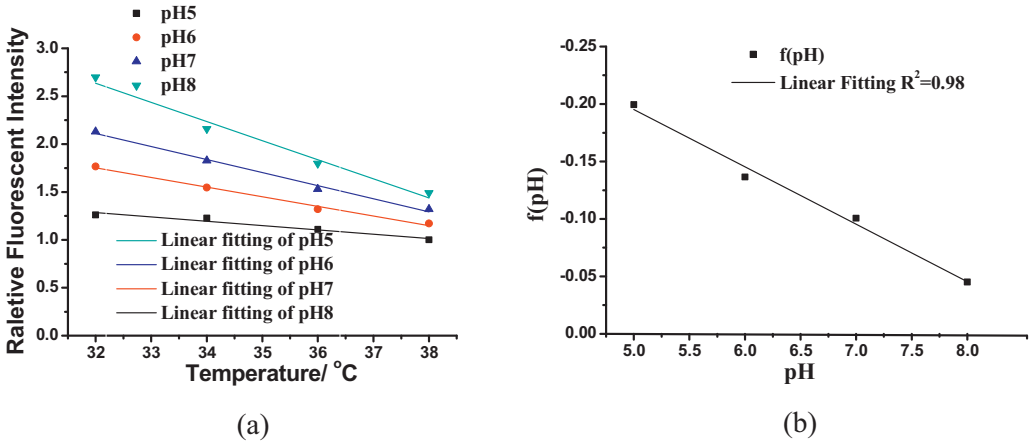

Fig. 7. (a) Responses of FITC to temperature at different pH values (5–8) (b) Temperature sensitivity of FITC at different pH values (5–8).

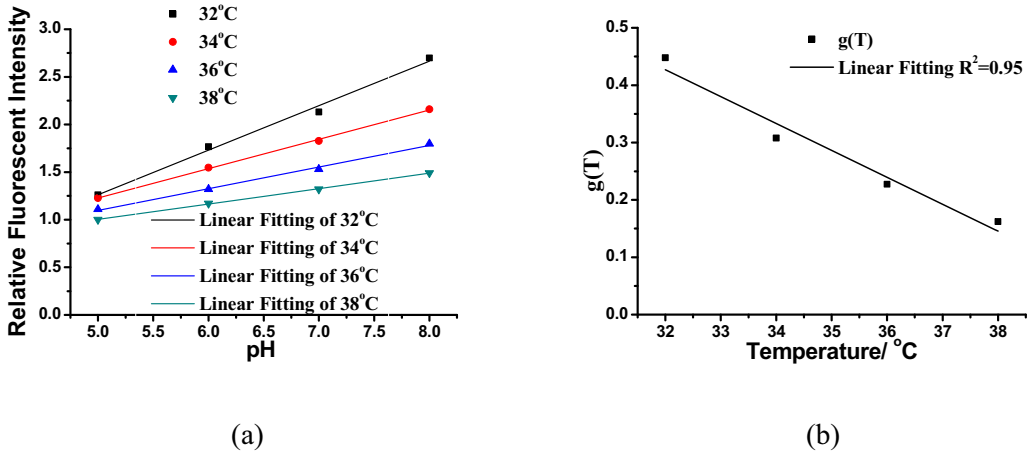

Fig. 8. (a) Responses of FITC to pH at different temperatures (32–38 °C) (b) pH sensitivity of FITC at different temperatures (32–38 °C).

3.2. Responses of Rhodamine B to pH and temperature

The fluorescence responses of Rhodamine B to pH and temperature were measured in different pH solutions and at different temperatures. We define the fluorescence intensity detected in a pH 5 solution at 32 °C as the basis point (F_0), and the relative fluorescence intensity (F) is the normalized value by comparing the measured fluorescence intensity (F_1) to the basis point (F_0). The unit of fluorescence intensity is arbitrary unit while the relative fluorescence intensity (F) is a non-dimensional value since it is the ratio of F_1 and F_0. ΔF is the change of relative fluorescence intensity (F), so ΔF is also a non-dimensional value.

As shown in Fig. 6, the relative fluorescence intensity of Rhodamine B decreased as the temperature increased, and the

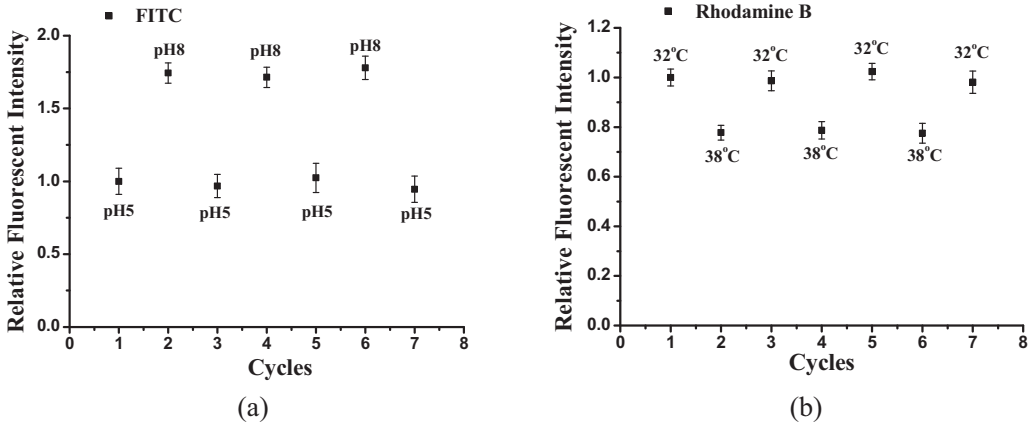

Fig. 9. Changes in the fluorescence intensity of the fluorescent sensor (a) for FITC (pH was repeatedly changed between 5 and 8 at 34 °C) (b) for Rhodamine B (temperature was changed repeatedly between 32 and 38 °C in a pH 7.4 solution).

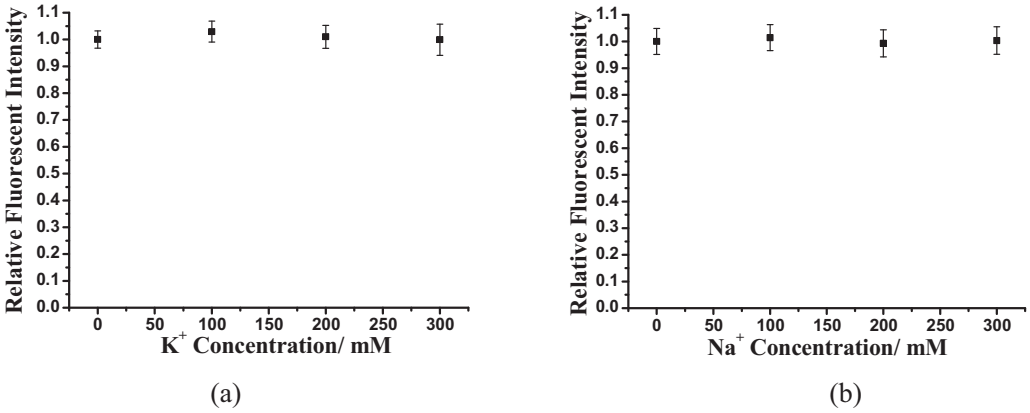

Fig. 10. Fluorescence responses of FITC in solutions (pH 7.4, 34 °C) with different ionic strengths: (a) K^+: 0, 100, 200, 300 mM (b) Na^+: 0, 100, 200, 300 mM.

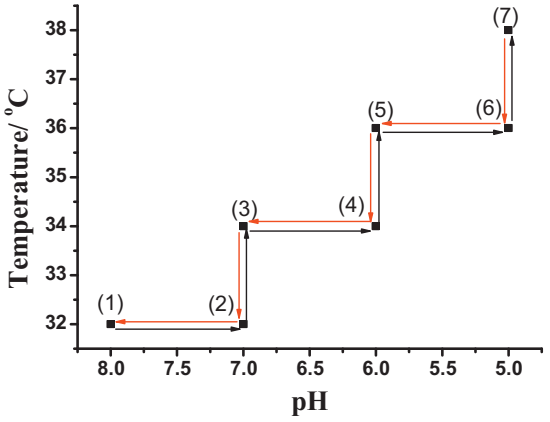

Fig. 11. Experimental order: (1) pH 8 and 32 °C, (2) pH 7 and 32 °C, (3) pH 7 and 34 °C, (4) pH 6 and 34 °C,(5) pH 6 and 36 °C, (6) pH 5 and 36 °C, (7) pH 5 and 38 °C, and the experimental cycle is changed from (1) to (7) and returned to (1).

sensitivities obtained in the different pH solutions were the same. It should be emphasized that Rhodamine B has an excellent linear relationship between its relative fluorescence intensity and temperature, and it is independent of pH [16]. Its relationship is shown in Eq. (2). The temperature information can be calibrated based on the fluorescence change in Rhodamine B using Eqs. (2) and (3).

$$\Delta F_{R(Rho.B)} = -0.034 \times \Delta T \quad (2)$$

$$T_2 = \frac{\Delta F_{R(Rho.B)}}{-0.034} + T_1 \quad (3)$$

where T_1 is the initial temperature, T_2 the temperature after change and ΔT is the temperature change.

3.3. Responses of FITC to pH and temperature

According to the measurement procedure, the temperature of the chamber was increased from 32 to 38 °C, and the fluorescence responses of FITC to temperature were measured in solutions with different pH values (5–8). Several curves of the relative fluorescence intensity based on the temperature in solutions with different pH values were obtained and are shown in Fig. 7. It can be seen in Fig. 7(a) that the relative fluorescence intensity of FITC decreases as the temperature increases in the range from 32 to 38 °C, and a linear relationship between the relative fluorescence intensity and temperature was found and is expressed as Eq. (4). After a linear fitting of Fig. 7(a), the temperature sensitivities of FITC are shown in Fig. 7(b). It should also be noted that the temperature sensitivities of FITC are dependent on the pH, and the temperature sensitivity f(pH) is expressed by Eq. (5). It should be emphasized that FITC is dependent on both temperature and pH.

Based on Fig. 7, the fluorescence responses of FITC to pH at different temperatures can also be obtained and are shown in Fig. 8. It is obvious that the pH sensitivity of FITC is also dependent on temperature. The pH information can be calibrated based on the relative fluorescence change of FITC using Eqs. (6) and (8), and

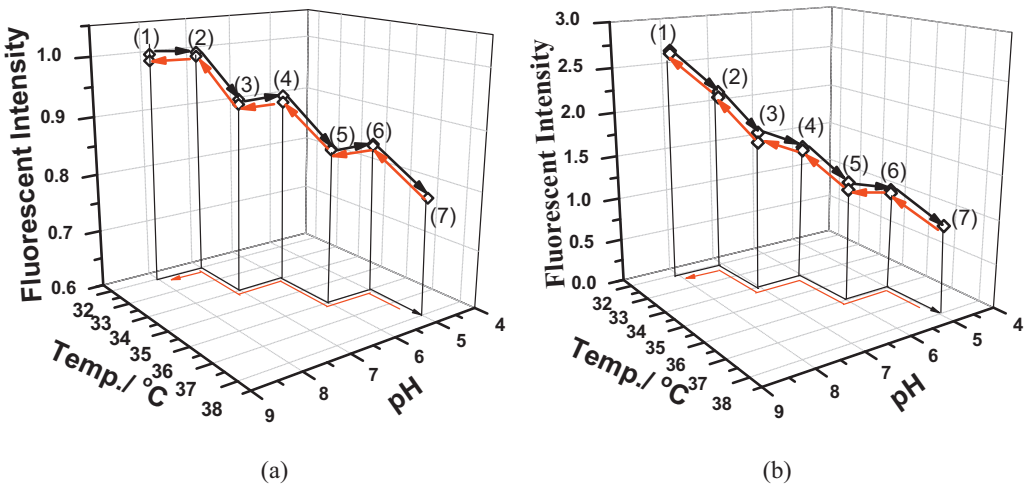

Fig. 12. Fluorescence responses of the sensor to pH and temperature changes (a) Rhodamine B (b) FITC (the experimental order is consistent with Fig. 11).

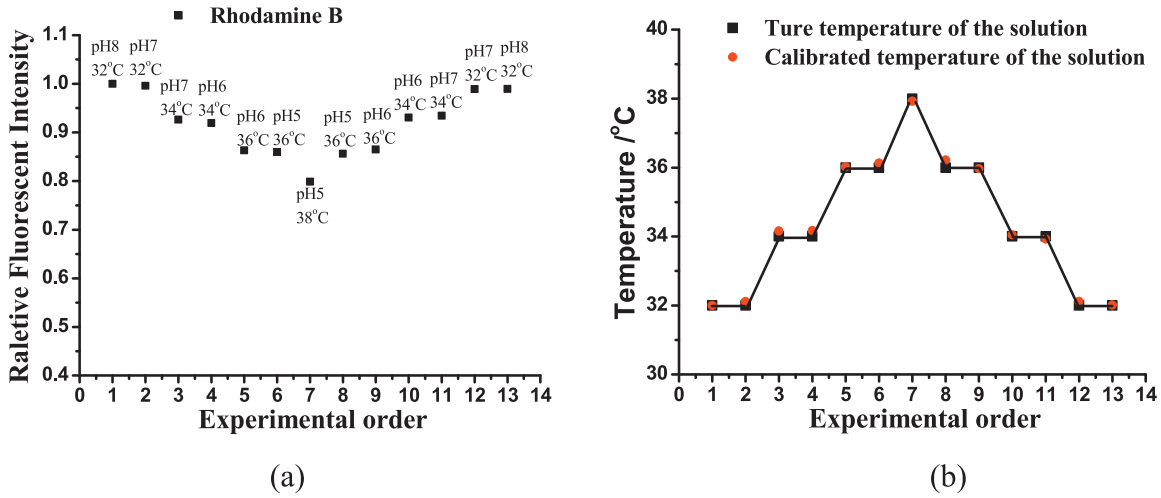

Fig. 13. (a) Fluorescence responses of Rhodamine B to temperature and pH (the experimental order is consistent with Fig. 9). (b) The measured and calibrated temperature values based on the fluorescence response results in (a).

the pH sensitivity, $g(T)$, related to temperature is expressed as Eq. (7). These linear relationships are necessary for the temperature compensation required for pH calibrations.

$$\Delta F_{R(FITC)} = f(\text{pH}) \times \Delta T \quad (4)$$

$$f(\text{pH}) = 0.0499 \times \text{pH} - 0.445 \quad (5)$$

$$\Delta F_{R(FITC)} = g(T) \times \Delta\text{pH} \quad (6)$$

$$g(T) = -0.047 \times \text{Temp.} + 1.93 \quad (7)$$

$$\text{pH}_2 = \Delta\text{pH} + \text{pH}_1 = \frac{\Delta F_{R(FITC)}}{g(T)^{+\text{pH}_1}} \quad (8)$$

where pH_1 is the initial pH value, pH_2 the pH value after change and ΔpH is the change in the pH value.

3.4. Reversibility of FITC and Rhodamine B fluorescence responses to pH and temperature

We also detected the reversibility of FITC and Rhodamine B fluorescence responses to pH and temperature, respectively. Fig. 9(a) shows the fluorescence intensity change in FITC when the pH is repeatedly changed between 5 and 8. The results show that the fluorescence intensity of FITC reversibly changes based on the pH through at least four cycles. Similarly, Fig. 9(b) shows the fluorescence intensity change in Rhodamine B when the temperature is repeatedly changed between 32 and 38 °C. The fluorescence intensity of Rhodamine B is also reversibly changeable for a minimum of four cycles upon temperature changes. This suggests that the fluorescent sensor possesses good reversibility towards pH and temperature changes.

3.5. Applicability of the multi-fluorescent micro-sensor to the surrounding ionic strength

Salt concentrations have been reported to influence the absorbance and emission spectra of pH indicators [17]. To examine the effect of ionic strength on the optical properties of the fluorescent micro-sensor, the fluorescence intensity of FITC was measured in buffer solutions containing different concentrations of KCl (0, 100, 200 and 300 mM) and NaCl (0, 100, 200 and 300 mM). FITC, which is on the surface of the micro-sensor, is likely to be affected by the surrounding ionic strength. The responses of FITC to different ionic strength solutions were detected, and the results are shown in Fig. 10 as the average of ten beads. The results show that there were no significant changes in the relative fluorescence intensity of FITC in solutions with different concentrations of K^+ and Na^+. The optical

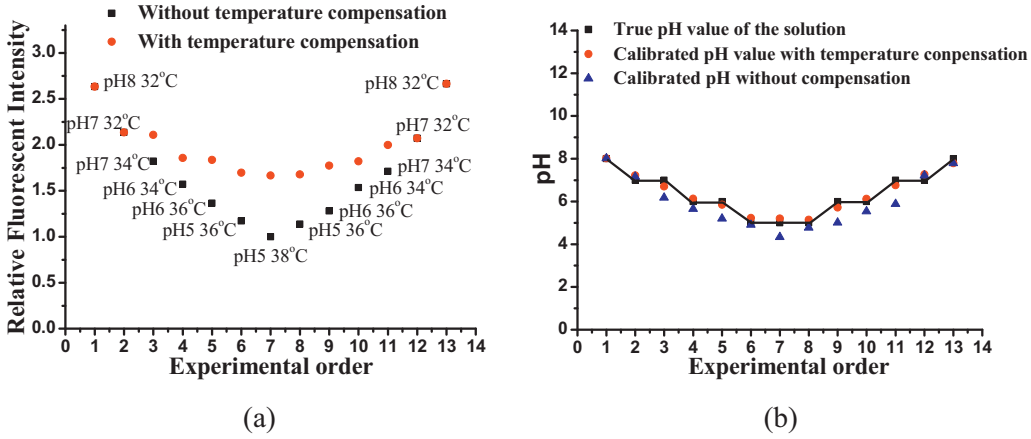

Fig. 14. (a) Fluorescence responses of FITC to temperature and pH (the experimental order is consistent with Fig. 9). (b) The measured and calibrated pH values based on the fluorescence response results in (a).

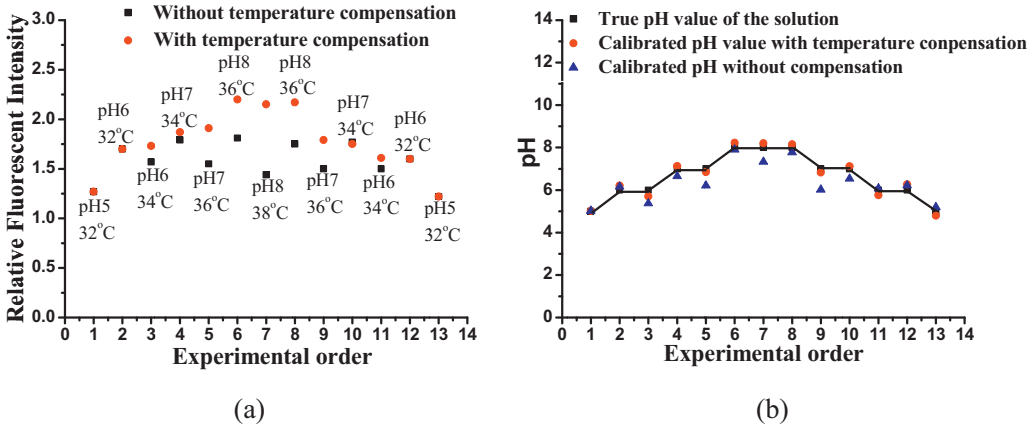

Fig. 15. (a) Fluorescence responses of FITC to temperature and pH (the pH value increases from 5 to 8 and then decreases to 5, which is contrary to the pH change order in Fig. 9). (b) The measured and calibrated pH values based on the fluorescence response results in (a).

properties of the fluorescent micro-sensor are not influenced by small changes in the ionic strength. This indicates that FITC is highly selective to pH and shows good applicability for pH sensing.

3.6. pH and temperature measurements by the micro-sensor using temperature compensation

In order to confirm the accuracy of the micro-sensor for pH and temperature change calibrations, the fluorescence responses of the sensor to changes in pH and temperature were measured. The pH values and temperature of the solution were changed as shown in Fig. 11 from (1) pH 8 and 32 °C to (7) pH 5 and 38 °C and then returned to (1) pH 8 and 32 °C. The fluorescence responses of Rhodamine B and FITC to pH and temperature changes are shown in Fig. 12. Fig. 12(a) shows that Rhodamine B only responds to temperature changes, which is consistent with the results in Fig. 6. Fig. 12(b) also shows that a decrease in pH or increase in temperature can induce a decrease in the fluorescence intensity of FITC. Moreover, it can also be seen in Fig. 12 that the fluorescence intensities of Rhodamine B and FITC return to their original values after the pH and temperature parameters return to (1).

Based on the measured relative fluorescence intensity changes in Fig. 12 and Eqs. (3) and (8), the temperature and pH values of the solutions can be calibrated. As shown in Fig. 13, based on the fluorescence changes in Rhodamine B, the temperature was calibrated using Eq. (3). Fig. 13(b) shows that the calibrated temperature values are consistent with the measured values, and the accuracy of the temperature calibration by Rhodamine B is within 0.1 °C. For FITC, which can respond to both pH and temperature changes, temperature compensation was necessary for pH calibration to remove any interference from its temperature response. Its fluorescence change with pH and temperature is shown by the black data in Fig. 14(a). The fluorescence change of FITC caused by temperature changes can be calibrated using Eq. (4). Once the fluorescence change caused by the temperature was added to the black data, the fluorescence change of FITC with temperature compensation is shown as the red data. Based on the results of the relative fluorescence intensity changes in Fig. 14(a) and Eq. (8), the pH values of the solution, with and without temperature compensation, were calibrated and are shown in Fig. 14(b). We changed the experimental order and repeated the pH calibration. The pH value increased from 5 to 8 and then decreased back to 5, which was contrary to the pH change order in Fig. 11, and the temperature was increased

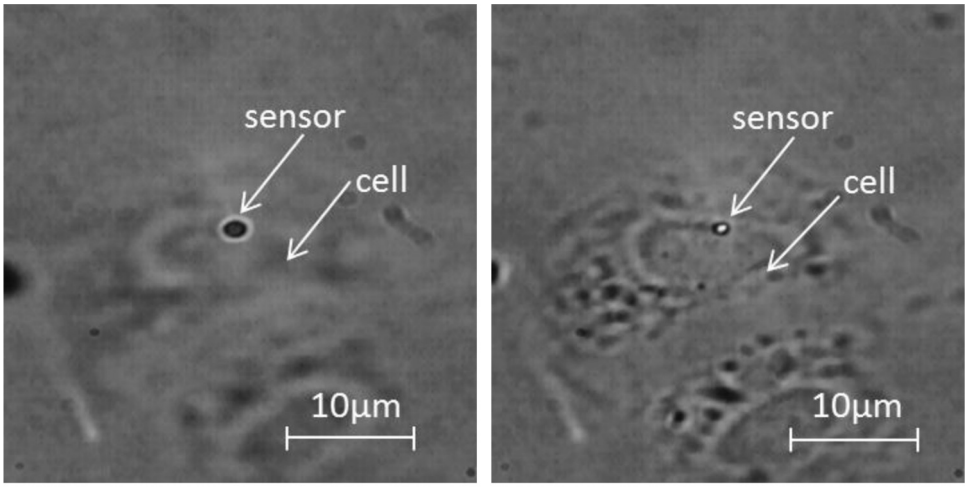

Fig. 16. One sensor on the surface of a MDCK cell (a) Before adhesion. (b) After adhesion.

from 32 to 38 °C and back to 32 °C. The fluorescence responses of FITC to pH and temperature, with and without temperature compensation, are shown in Fig. 15(a), and the calibrated pH values based on the fluorescence changes of FITC are shown in Fig. 15(b). It is clear that the calibrated pH value with temperature compensation is consistent with the measured value. After temperature compensation by our proposed method, the pH accuracy based on the calibrated fluorescence change of FITC was improved from 1.5 to 0.2.

4. The feasibility of applying the micro-sensor in cell measurement

As we know virus infected cells [18,19] show different pH value comparing with that of normal cells. So succeeding in measuring the temperature and pH changes of these cells can help us to understand physiological and pathological processes of many diseases. In this paper, we propose that the fabricated multi-fluorescent micro-sensor based on polymeric microbeads can be applied in cell measurement in biological and medical applications.

In a real scenario, the sensor can be used in cells after sensitivity calibration. Firstly, a single sensor with a diameter of 1 μm is successfully controlled and manipulated by optical tweezers. It can be transferred and adhere to the surface of a MDCK cell, as shown in Fig. 16. In order to monitor the intracellular temperature and pH change, it is necessary to inject the sensor into a single cell. There are many technologies for sensor injection, for example, microinjection using micro-nano pipette [20], non-invasive methods such as endocytosis and lipofection [21], mechanical stimulus on the sensor [22], and so on. So it is possible to measure the intracellular environmental changes. Actually, we always culture the cells in cell culture dish in incubator with a condition of 37 °C and CO_2 level of 5%. The medium pH as well as intracellular pH (cytoplasm) is about 7.4. So the initial condition of temperature and pH is already known before any changes happen in the cells. If any relative fluorescence change can be monitored, the temperature and pH changes can be calibrated. Furthermore, based on Eqs. (3) and (8) which have been shown in the paper, the absolute temperatures and pH values can also be calibrated. It is anticipated to show cell measurement results in the near future.

5. Conclusions

We synthesized a novel multi-fluorescent micro-sensor based on polymeric microbeads that can simultaneously support pH and temperature sensitive FITC dye and temperature sensitive Rhodamine B dye on a single particle. Rhodamine B possesses high fluorescence emission at an excitation wavelength of 561 nm and shows good fluorescence responses to temperature in the range of 32–38 °C. The calibrated sensitivity of Rhodamine B is −3.4%/°C, with a temperature accuracy of 0.1 °C. FITC possesses high fluorescence emission at an excitation wavelength of 488 nm and shows good fluorescence responses to solution pH. Because temperature can also affect the fluorescence change of FITC, we proposed a method to perform a temperature compensation for pH calibration. After the temperature compensation by our proposed method, the calibrated pH value based on the fluorescence change in FITC was consistent with the measured value. The pH accuracy was improved from 1.5 to 0.2. Using this micro-sensor, pH and temperature changes can be calibrated. This micro-sensor has high selectivity for pH and temperature, good stability, and a high tolerance for ionic strength, making it suitable for cellular measurements. The sensor is based on a single microbead, which would only be a small stimulus to cells and could also detect the local cell conditions. For cell measurements, the biocompatibility of this sensor will be investigated in future. On the other hand, the novel fluorescent micro-sensor not only can be used in cell measurement, but also sensing in other close micro-environments, such as micro chamber and microfluidic chip. It can provide low contamination and high accuracy for local condition measurement in micro-environments.

Acknowledgements

This work has been supported by Core Research for Evolutional Science and Technology (CREST) of JST.

References

[1] K. Okabe, N. Inada, C. Gota, Y. Harada, T. Funatsu, S. Uchiyama, Intracellular temperature mapping with a fluorescent polymeric thermometer and fluorescence lifetime imaging microscopy, Nat. Commun. 3 (2012), No. 705.
[2] A. Ishaque, M. Al-Rubeai, Use of intracellular pH and annexin-V flow cytometric assays to monitor apoptosis and its suppression by bcl-2 over-expression in hybridoma cell culture, J. Immunol. Methods 221 (1998) 43–57.
[3] R.A. Gottlieb, J. Nordberg, E. Skowronski, B.M. Babior, Apoptosis induced in Jurkat cells by several agents is preceded by intracellular acidification, Proc. Natl Acad. Sci. U.S.A. 93 (1996) 654–658.
[4] J. Qiao, L. Qi, Y. Shen, L.Z.H. Zhao, C. Qi, D.H. Shangguan, L.Q. Mao, Y. Chen, Thermal responsive fluorescent block copolymer for intracellular temperature sensing, J. Mater. Chem. 22 (2012) 11543–11549.
[5] P. Breedveld, D. Pluim, G. Cipriani, F. Dahlhaus, M.A. van Eijndhoven, C.J. de Wolf, A. Kuil, et al., The effect of low pH on breast cancer resistance protein (ABCG2)-mediated transport of methotrexate, 7-hydroxymethotrexate, methotrexate diglutamate, folic acid, mitoxantrone, topotecan, and resveratrol in in vitro drug transport models, Mol. Pharmacol. 71 (2007) 240–249.
[6] D. Lindne, D. Raghavan, Intra-tumoural extra-cellular pH: a useful parameter of response to chemotherapy in syngeneic tumour lines, Brit. J. Cancer 100 (2009) 1287–1291.
[7] H. Maruyama, T. Otake, F. Arai, Photoprocessible hydrogel microsensor for local environment measurement on a microfluidic chip, IEEE-ASME T. Mech. 16 (2011) 845–852.
[8] S. Nagl, O.S. Wolfbeis, Optical multiple chemical sensing: status and current challenges, Analyst 132 (2007) 507–511.
[9] S.M. Borisov, C. Krause, S. Arain, O.S. Wolfbeis, Composite material for simultaneous and contactless luminescent sensing and imaging of oxygen and carbon dioxide, Adv. Mater. 18 (2006) 1511–1516.
[10] A. Al Salman, A. Tortschanoff, M.B. Mohamed, A.D. Tonti, B.F. van Mourik, M. Cherguic, Temperature effects on the spectral properties of colloidal CdSe nanodots, nanorods, and tetrapods, Appl. Phys. Lett. 90 (2007), 093104–093104-3.
[11] J.Y. Han, K. Burgess, Fluorescent indicators for intracellular pH, Chem. Rev. 110 (2010) 2709–2728.
[12] L.Y. Yin, C.S. He, C.S. Huang, W.P. Zhu, X. Wang, Y.F. Xu, X.H. Qian, A dual pH and temperature responsive polymeric fluorescent sensor andits imaging application in living cells, Chem. Commun. 48 (2012) 4486–4488.
[13] Y.H. Liu, T.H. Dam, P. Pantano, A pH-sensitive nanotip array imaging sensor, Anal. Chim. Acta 419 (2000) 215–225.
[14] Y.Y. Li, H. Cheng, J.L. Zhu, L.Y.Y. Dai, S.X. Cheng, X. Zh Zhang, R.X. Zhuo, Temperature- and pH-sensitive multicolored micellar complexes, Adv. Mater. 21 (2009) 2402–2406.
[15] H. Maruyama, R. Kariya, S. Nakamura, T. Matsuda, Yu Matsuda, A. Honda, F. Arai, Ultra long-lifetime and high-sensitive fluorescent measurement using difference compensation method for single cell analysis, in: IEEE/RSJ International Conference on Intelligent Robots and Systems (2012), 3235–3240.
[16] H. Maruyama, T. Fukuda, F. Arai, Functional gel-microbead manipulated by optical tweezers for local environment measurement in microchip, Microfluid. Nanofluid. 6 (2009) 383–389.
[17] J. Zhou, C.L. Fang, T.J. Chang, X.J. Liu, D.H. Shangguan, A pH sensitive ratiometric fluorophore and its application for monitoring the intracellular and extracellular pHs simultaneously, J. Mater. Chem. B 1 (2013) 661–667.
[18] F. Ciampor, C.A. Thompson, S. Grambas, A.J. Hay, Regulation of pH by the M2 protein of influenza A viruses, Virus Res. 22 (1992) 247–258.
[19] L.L. Moore, D.A. Bostick, R.F. Garry, Sindbis virus infection decreases intracellular pH: alkaline medium inhibits processing of sindbis virus polyproteins, Virology 166 (1988) 1–9.
[20] H. Maruyama, N. Inoue, T. Masuda, F. Arai, Selective injection and laser manipulation of nanotool inside a specific cell using optical pH regulation and optical tweezers, Proc. ICRA (2011), 2674-2679.
[21] J. Edahiro, K. Sumaru, Y. Tada, K. Ohi, T. Takagi, M. Kameda, T. Shinbo, T. Kanamori, Y. Yoshimi, In situ control of cell adhesion using photoresponsive culture surface, Biomacromolecules 6 (2005) 970–974.
[22] S.T. Truschel, E. Wang, W.G. Ruiz, S.M. Leung, R. Rojas, J. Lavelle, M. Zeidel, D. Stoffer, G. Apodaca, Stretch-regulated exocytosis/endocytosis in bladder umbrella cells, Mol. Biol. Cell 13 (2002) 830–846.

Biographies

Hengjun Liu is currently working toward the Ph.D. degree for micro-nano systems engineering at Arai Laboratory, Nagoya University, Nagoya 464-8603, Japan. She received master degree in Biomedical Engineering in 2011, Southwest Jiaotong University, Chengdu 610031, China. Her current research interests are micro-nano sensors and actuators and micro-nano manipulation including optical control system, on-chip robotics (laser driven type).

Hisataka Maruyama is Associate Professor at the Graduate School of Engineering, Nagoya University, Japan. He obtained his Ph.D. in micro-nano system engineering from the Graduate School of Engineering, Nagoya University, Japan. His research field is in the micro-nano robotics, micro-nano manipulation, micro-nano sensors and actuators.

Taisuke Masuda is an Assistant Professor at the Graduate School of Engineering, Nagoya University, Japan. He obtained his Ph.D. in engineering from the Graduate School of Engineering, Oita University, Japan. His research area has been in the biomedical engineering and bio MEMS.

Ayae Honda is Professor at the department of Frontier Bioscience, Hosei University, Tokyo, Japan. She is mainly engaging in the research fields of molecular biology, especially in the research of virus infection on to a single cell for monitoring single virus, transportation of viral RNP in nucleus and manipulation of chromosome using optical tweezers.

Fumihito Arai is Professor at the Graduate School of Engineering, Nagoya University, Japan. He is mainly engaging in the research fields of micro- and nano-robotics and its application to the micro- and nano-assembly and cell manipulation, bio-automation systems, medical robotic systems, micro and nano electro mechanical systems, intelligent robotic systems.